# A direct method for the location of the lowest energy point on a potential surface crossing

Michael J. Bearpark [a], Michael A. Robb [a], H. Bernhard Schlegel [b]

[a] *Department of Chemistry, King's College, London, Strand, London WC2R 2LS, UK*
[b] *Department of Chemistry, Wayne State University, Detroit, MI 48202, USA*

Received 31 March 1994; in final form 18 April 1994

## Abstract

We present a method, which avoids the use of Lagrange multipliers, for the optimisation of the lowest energy point of the intersection of two potential energy surfaces. The efficiency of this unconstrained algorithm is demonstrated for the $n-2$ intersection space of a conical intersection and the $n-1$ intersection space of the crossing of two states of different spin multiplicity.

## 1. Introduction

Recently, it has been demonstrated (see refs. [1–16] for examples) that the characterisation of surface crossings [17–23] has an important role to play in the investigation of the mechanism of photochemical reactions. Such crossings serve as funnels [21,22] where transitions from one state to another are most likely to take place.

Practical algorithms for the investigation of surface crossings have only begun to emerge [24–28] in recent years. These use analytic gradient methods with constraints incorporated via the method of Lagrange multipliers. The method described by Mana and Yarkony [27] also requires the Hessian of the Lagrangian, which is evaluated numerically. The purpose of the present Letter is to outline an efficient method for the location of surface crossings that is *direct* in the sense that no constraints are used. As a consequence, the normal Hessian updating methods that are used in a program such as GAUSSIAN 92 [29] work without modification and the optimisation of the surface crossing region becomes possible without computing the Hessian [27] in the space of nuclear displacements.

## 2. Theoretical development

Two states, even with the same symmetry, may intersect along an $(n-2)$-dimensional hyperline as the energy is plotted against the $n$ nuclear co-ordinates. Such an intersection is a conical intersection [17–23]. If the two states have different spin multiplicity, this intersection reduces to an $(n-1)$-dimensional hyperline. The optimisation of the lowest energy point on such hyperlines can be carried out with one constraint [24,26] or two constraints [27].

At a conical intersection, one can distinguish two directions, $x_1$ and $x_2$, such that if one were to plot the energy in the subspace of these two geometric variables (combinations of the bond lengths, angles, etc.) the potential energy would have the form of a double cone in the region of the degeneracy. In the remaining $n-2$ directions, the energies of ground and excited states are equal; movement in the plane $x_1$ and

$x_2$ lifts this degeneracy. At the lowest energy point on this hyperline, the energy of the excited state is minimised in $n-2$ variables and the gradient of the excited state potential energy surface is zero in the $(n-2)$-dimensional space orthogonal to $x_1$ and $x_2$. The vectors $x_1$ and $x_2$ lie parallel to the gradient difference vector

$$x_1 = \frac{\partial(E_1 - E_2)}{\partial q} \tag{1}$$

and the gradient of the interstate coupling vector

$$X_2 = \left\langle C_1^t \left( \frac{\partial H}{\partial q} \right) C_2 \right\rangle , \tag{2}$$

where $C_1$ and $C_2$ are the CI eigenvectors in an MC-SCF or CI problem.

The optimisation of the lowest energy point on a surface crossing is defined by requiring that the energy is minimised in the $(n-2)$-dimensional space orthogonal to the plane $x_1$ and $x_2$ and that $E_1 = E_2$. One can either optimise $E_2$ subject to 2 constraints [27] or one may simultaneously minimise the energy difference $E_1 - E_2$ in the plane spanned by $x_1$ and $x_2$, and minimise $E_2$ in the remaining $(n-2)$-dimensional space orthogonal to the $x_1, x_2$ plane. The latter approach yields an unconstrained method that does not require Lagrange multipliers. The purpose of this Letter is to document the second unconstrained approach.

The condition chosen for the minimisation of $E_1 - E_2$ in the $x_1, x_2$ plane is

$$\frac{\partial}{\partial q_\alpha} (E_2 - E_1)^2 = 2(E_2 - E_1)x_1 = 0 , \tag{3}$$

where $x_1$ is the gradient difference vector defined in Eq. (1). Because $(E_1 - E_2)^2$ varies more smoothly than $E_1 - E_2$ in the vicinity of the conical intersection, this approach is more suitable for quasi-Newton minimisation methods. The length of $x_1$ has no significance – only its direction. ($|x_1|$ will be large if the potential energy surfaces have opposite slope but very small if they have nearly the same slope.) This means that the size of the step should only depend upon $E_1 - E_2$, and suggests that we should take the gradient along the step to the minimum of $E_1 - E_2$ to be

$$f = 2(E_2 - E_1) \frac{x_1}{\sqrt{x_1 \cdot x_1}} . \tag{4}$$

Clearly $f$ will go to zero when $E_2 = E_1$, independently of the magnitude of $x_1$. If we now define the projection $P$ of the gradient of $E_2$ onto the $n-2$ orthogonal complement to the plane $x_1 x_2$ as

$$g = P \frac{\partial E_2}{\partial q_\alpha} , \tag{5}$$

then the gradient to be used in the optimisation becomes

$$\bar{g} = g + f . \tag{6}$$

In the case where $x_2$ is zero because we have two states of different spin multiplicity, we simply project onto the $(n-1)$-dimensional orthogonal complement space. This algorithm is similar in spirit to MC-SCF optimisation where one is optimising both the orbital rotations and the CI vector. One of the principle advantages of the technique just discussed arises from the fact that as $f$ goes to zero the normal Hessian updating should ensure efficient convergence.

From a practical point of view the preceding algorithm is easily implemented within the context of MC-SCF theory. We have simply used the procedure outlined by Yarkony [30] for the computation of gradient difference and non-adiabatic coupling matrix elements using state-averaged orbitals. Because the procedure requires the solution of the coupled perturbed state-averaged MC-SCF equations at each iteration, such optimisations are very expensive. However, in practice the contributions that arise from the derivatives of the orbital rotations are quite small, and the initial iterations can be carried out quite cheaply if these contributions are neglected [26].

## 3. Some numerical examples

The purpose of this section is to illustrate the convergence characteristics of the unconstrained minimisation algorithm for $(n-2)$- and $(n-1)$-dimensional crossing surfaces in benzene. To illustrate the global convergence of the method, the minimum energy point on the $n-2$ intersection of the $S_0$ and $S_1$ states of benzene has been optimised. This conical intersection has been previously documented [8,13,14] and forms the mechanism of the 'channel 3' decay process from the $S_1$ state of benzene. As an example of an $n-1$ crossing, we have computed the

minimum energy point on the intersection of the $S_0$ and $T_1$ states of benzene. This crossing provides a mechanism for the chemiluminescence of Dewar benzene [31].

We begin with a discussion of the global convergence of a conical intersection optimisation of the $n-2$ intersection of the $S_0$ and $S_1$ states of benzene. Normally, one might have a rather good estimate of the geometry of a conical intersection by performing grid searches etc. Our purpose here is to illustrate that the direct method proposed in this Letter has quite a large radius of convergence. Thus the computations have been started rather a long way from the target minimum (near to the benzene $S_0$ minimum, with one carbon atom slightly displaced out of plane to remove the planar constraint). Since our purpose is only to illustrate global convergence (involving a very large number of iterations) we have used a crude STO-3G basis and a 6 in 6 CASSCF.

In Fig. 1 we show the energy separation and geometry change during the optimisation of the $n-2$ conical intersection of the $S_0$ and $S_1$ states of benzene. In Fig. 2 we show the corresponding behaviour of the RMS values of (i) the projection of the gradient of $E_2$ onto the $n-2$ orthogonal complement to the plane $x_1x_2$ defined by Eq. (5) and (ii) the overall gradient used in the optimisation defined by Eq. (6).
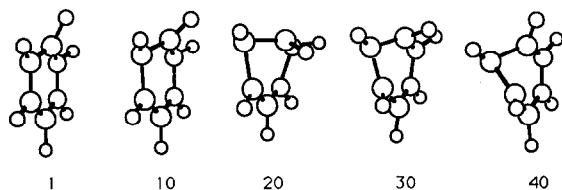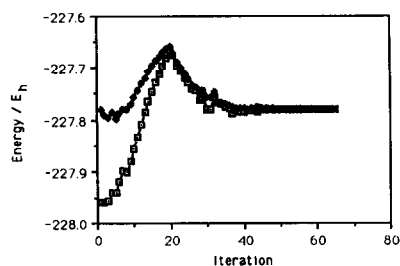


Fig. 1. Global convergence (CAS(6,6)/STO-3G) of an optimisation of the $S_0/S_1$ conical intersection of benzene. Geometries for selected points along the optimisation path are shown at the bottom of the figure. ($\square$) $S_0$, ($\blacklozenge$) $S_1$.
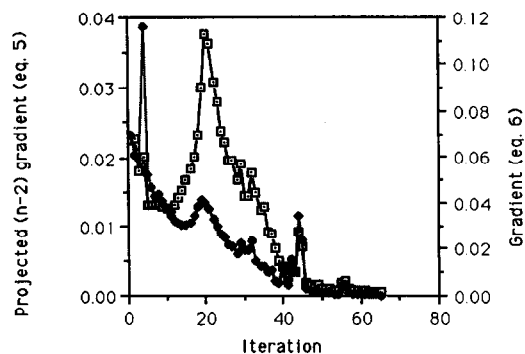


Fig. 2. The RMS projected $n-2$ gradient (left axis), Eq. (5), and the RMS gradient (right axis), Eq. (6), for the $S_0/S_1$ benzene conical intersection optimisation. ($\square$) Projected $n-2$ gradient, ($\blacklozenge$) gradient.

In our experience, this convergence pattern is typical. The initial phase of the optimisation is dominated by steps leading to $E_2 = E_1$. When the energy difference is large the gradient is dominated by the gradient difference vector defined in Eq. (4). Thus during the first 20 iterations, the energy difference decreases until the two states become nearly degenerate, and one has moved to an arbitrary point on the $(n-2)$-dimensional hyperline. However, this geometry is far from the minimum on this hyperline and one can see that the geometry is rather distorted (four of the C–C bonds have been stretched to greater than 1.6 Å). Further, the projected gradient of $E_2$ onto the $n-2$ orthogonal complement (Eq. (5)) is a maximum at iteration 20. However, notice that the overall gradient (Eq. (6)) is steadily decreasing. For the remaining 50 iterations the projected gradient of $E_2$ decreases continuously (Fig. 2) and the energy of $E_2 = E_1$ also decreases. Thus the final phase looks more or less like a typical geometry optimisation (that has been started from a very poor initial guess). In this phase the usual updating methods perform well.

Of course the detailed behaviour of the algorithm depends upon the choice of geometric variables, the method of Hessian updating, etc. One would not normally contemplate performing a geometry optimisation with such a poor initial geometry. However, our purpose here is merely to demonstrate convergence under extreme conditions. Further, optimising 'floppy' rings in internal coordinates is always difficult. There is obviously room for 'fine tuning' improvements. In particular, from Fig. 2 it is apparent

that there is room to 'tune' the balance between stepping toward the intersection and stepping toward the minimum by scaling $f$ (Eq. (4)) by a number less than 1 that does not compromise on the convergence of $E_1 - E_2$. This approach could also eliminate the possible imbalance between the force constants in the $x_1, x_2$ space so that the final phase of the optimisation converges more rapidly. We have used a crude STO-3G basis in the interests of economy for this test. However, this does not invalidate the general arguments just outlined. The final geometry – shown in Fig. 3 – is almost identical to that obtained previously [8] with the 4-31G basis, and the optimisation algorithm described in ref. [26].

We now turn to a second example that illustrates a different aspect of our algorithm: the $(n-1)$-dimensional crossing between the $S_0$ and $T_1$ states of benzene. Turro [31] has suggested that the mechanism of the chemiluminescence of Dewar benzene involves an $S_0/T_1$ crossing near the thermal transition state connecting Dewar benzene and benzene itself. In other words, the $T_1$ state of benzene cuts the $S_0$ surface near the transition state energy profile, providing a thermal route to the $T_1$ state of benzene which then emits. While we have characterised the thermal transition state in other work [8], the crossing mechanism has not previously been characterised.

The optimised geometry (CAS(6,6)/4-31G) of the lowest point on the $(n-1)$-dimensional crossing between the $S_0$ and $T_1$ states is shown in Fig. 4. While the thermal transition state is a 'boat-like' structure with a bridge head C–C distance of 2.24 Å, the $S_0/T_1$ crossing is a 'half-boat' with slightly broken symmetry. While this structure has some interest chemically, our purpose here is to make some theoretical
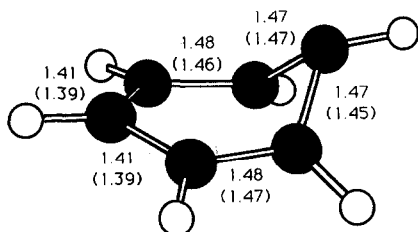


Fig. 4. The CAS(6,6)/4-31G optimised geometry of the $n-1$ intersection between the $S_0$ and $T_1$ states of benzene.

observations. Firstly, the optimisation method for an $(n-1)$-dimensional crossing behaves in a similar manner to the $(n-2)$-dimensional algorithm. Secondly, this example presents a rather special difficulty that one occasionally encounters in this type of problem which merits discussion.

At a crossing minimum, the gradients of the two surfaces are often of similar magnitude but opposite in sign. In fact, this was the case for the $S_0/S_1$ crossing. However, the gradients of the two surfaces can be nearly parallel. (If they are both zero then one has an avoided crossing minimum; the present algorithm can also handle this case, but we shall not consider it here.) Clearly if the surfaces are nearly parallel, then the magnitude of the gradient difference vector is very small. When this happens, the geometry of the crossing minimum is not well defined. In Fig. 5 we illustrate the gradient vectors of the $S_0$ and $T_1$ states at the crossing minimum. Indeed, they are almost identical at the crossing point. As a consequence, we needed to restrict the maximum stepsize to 0.01 Å during to optimisation and the RMS force could only be converged to 0.0025 with a final energy difference of 0.002 $E_h$. (In contrast, for the $S_0/S_1$ intersection search, the RMS force was less than 0.0003 with a final energy difference of 0.0001 $E_h$.) The slight asymmetry in the structure shown in Fig. 4 is a reflection of this low accuracy. However, this result is not a comment on the efficiency of the method used but rather represents a fundamental limitation on the accuracy that can be obtained.



Fig. 3. Final geometry of the $S_0/S_1$ conical intersection. Distances in Å. Bracketed geometry taken from ref. [8] (which used a 4-31G basis and the optimisation algorithm described in ref. [26].)
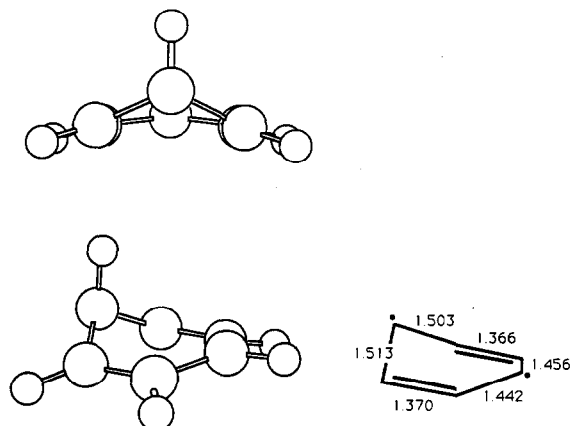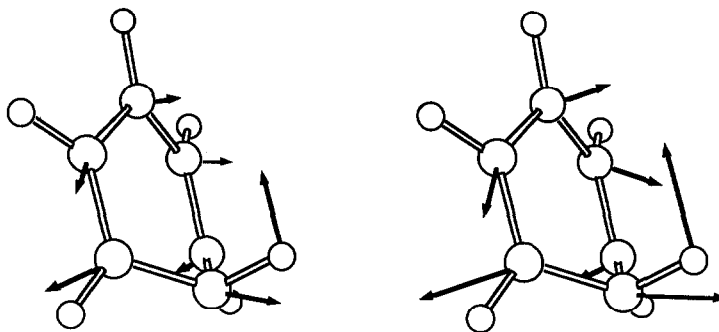
Fig. 5. The gradients of the $S_0$ (left) and $T_1$ (right) states at the optimised intersection geometry shown in Fig. 3.

## 4. Conclusions

An unconstrained algorithm for optimising critical points on the crossing surfaces of states of the same or different symmetries has been described. The optimisation of the $S_0/S_1$ conical intersection of benzene from a very poor starting geometry demonstrates the robust global convergence and the termination properties of the algorithm. The optimisation of $S_0/T_1$ intersection illustrates that the method can be used for an $(n-1)$-dimensional crossing but that problems must be expected when the two surfaces are nearly parallel.

## Acknowledgement

## References

[1] F. Bernardi, S. De, M. Olivucci and M.A. Robb, J. Am. Chem. Soc. 112 (1990) 1737.

[2] F. Bernardi, M. Olivucci and M.A. Robb, Accounts Chem. Res. 23 (1990) 405.

[3] F. Bernardi, M. Olivucci, I.N. Ragazos and M.A. Robb, J. Am. Chem. Soc. 114 (1992) 2752.

[4] F. Bernardi, M. Olivucci, M.A. Robb and G. Tonachini, J. Am. Chem. Soc. 114 (1992) 5805.

[5] F. Bernardi, M. Olivucci, I.N. Ragazos and M.A. Robb, J. Am. Chem. Soc. 114 (1992) 8211.

[6] I. Palmer, F. Bernardi, M. Olivucci and M.A. Robb, J. Org. Chem. 57 (1992) 5081.

[7] M. Olivucci, I.N. Ragazos, F. Bernardi and M.A. Robb, J. Am. Chem. Soc. 114 (1992) 8211.

[8] I.J. Palmer, I.N. Ragazos, F. Bernardi, M. Olivucci and M.A. Robb, J. Am. Chem. Soc. 115 (1993) 673.

[9] M. Reguero, F. Bernardi, H. Jones, M. Olivucci and M.A. Robb, J. Am. Chem. Soc. 115 (1993) 2073.

[10] M. Olivucci, I.N. Ragazos, F. Bernardi and M.A. Robb, J. Am. Chem. Soc 115 (1993) 3710.

[11] F. Bernardi, M. Olivucci and M.A. Robb, Israel J. Chem. 33 (1993) 256.

[12] M. Olivucci, F. Bernardi, I. Ragazos and M.A. Robb, J. Am. Chem. Soc. 116 (1994) 1077.

[13] W. Domke, A.L. Sobolewski and C. Woywod, Chem. Phys. Letters 203 (1993) 220.

[14] A.L. Sobolewski, C. Woywod and W. Domcke, J. Chem. Phys. 98 (1993) 5627.

[15] C. Woywood, W. Domcke, A.L. Sobolewski and H.J. Werner, J. Chem. Phys. 100 (1994) 1400.

[16] D.R. Yarkony, J. Chem. Phys. 100 (1994) 3639.

[17] L. Salem, Electrons in chemical reactions: first principles (Wiley, New York, 1982).

[18] J. von Neumann and E. Wigner, Physik. Z. 30 (1929) 467.

[19] E. Teller, J. Phys. Chem. 41 (1937) 109.

[20] G. Herzberg and H.C. Longuet-Higgins, Trans. Faraday Soc. 35 (1963) 77.

[21] W. Gerhartz, R.D. Poshusta and J. Michl, J. Am. Chem. Soc. 99 (1977) 4263.

[22] J. Michl and V. Bonacic-Koutecky, Electronic aspects of organic photochemistry (Wiley, New York, 1990).

[23] V. Bonacic-Koutecky, J. Koutecky and J. Michl, Agnew. Chem. Intern. Ed. Engl. 26 (1987) 170.

[24] N. Koga and K. Morokuma, Chem. Phys. Letters 119 (1985) 371.

[25] P.J. Kuntz and J.W.H. Whitton, Chem. Phys. 95 (1991) 5149.

[26] I.N. Ragazos, M.A. Robb, F. Bernardi and M. Olivucci, Chem. Phys. Letters 197 (1992) 217.

[27] M.R. Mana and D.R. Yarkony, J. Chem. Phys. 99 (1993) 5251.

[28] D.R. Yarkony, J. Phys. Chem. 97 (1993) 4407.

[29] M.J. Frisch, G.W. Trucks, M. Head-Gordon, P.M.W. Gill, M.W. Wong, J.B. Foresman, B.G. Johnson, H.B. Schlegel, M.A. Robb, E.S. Replogle, R. Gomperts, J.L. Andres, K.

Raghavachari, J.S. Binkley, C. Gonzalez, R.L. Martin, D.J. Fox, D.J. DeFrees, J. Baker, J.J.P. Stewart and J.A. Pople, GAUSSIAN 92, Revision B (Gaussian, Pittsburgh, 1992).

[30] D.R. Yarkony, J. Chem. Phys. 92 (1990) 2457.

[31] N.J. Turro, Modern molecular photochemistry (Benjamin Cummings, Menlo Park, 1978) p. 602.